

# Micromachined III–V cantilevers for AFM-tracking scanning Hall probe microscopy

A J Brook<sup>1</sup>, S J Bending<sup>1</sup>, J Pinto<sup>1</sup>, A Oral<sup>2</sup>, D Ritchie<sup>3</sup>, H Beere<sup>3</sup>,  
A Springthorpe<sup>4</sup> and M Henini<sup>5</sup>

<sup>1</sup> Department of Physics, University of Bath, Bath BA2 7AY, UK

<sup>2</sup> Department of Physics, Bilkent University, 06533 Ankara, Turkey

<sup>3</sup> Cavendish Laboratory, Cambridge University, Cambridge CB3 0HE, UK

<sup>4</sup> Nortel Networks Optical Components Inc., 3500 Carling Avenue, Ottawa, Ontario, Canada, K2H 8E9

<sup>5</sup> Department of Physics, University of Nottingham, Nottingham NG7 2RD, UK

Received 27 August 2002, in final form 8 November 2002

Published 4 December 2002

Online at [stacks.iop.org/JMM/13/124](http://stacks.iop.org/JMM/13/124)

## Abstract

In this paper we report the development of a new III–V cantilever-based atomic force sensor with piezoresistive detection and an integrated Hall probe for scanning Hall probe microscopy. We give detailed descriptions of the fabrication process and characterization of the new integrated sensor, which will allow the investigation of magnetic samples with no sample preparation at both room and cryogenic temperatures. We also introduce a novel piezoresistive material based on the ternary alloy  $n^+ \text{Al}_{0.4}\text{Ga}_{0.6}\text{As}$  which allows us to achieve a cantilever deflection sensitivity  $\Delta R/(R\Delta z) = 2 \times 10^{-6} \text{ \AA}^{-1}$  at room temperature.

## 1. Introduction

Since its invention, the magnetic force microscope (MFM) [1] has been widely used as a simple technique for the investigation of stray fields at the surface of magnetic samples with sub-micron resolution. However, the technique can be invasive and non-quantitative, which has led to the development of alternative magnetic imaging methods. One complementary technique, which is both non-invasive and quantitative, is the scanning Hall probe microscope (SHPM), which is capable of magnetic imaging at spatial resolutions down to 150 nm [2–4]. A SHPM commonly uses an integrated scanning tunnelling microscope (STM) tip to bring the Hall probe into close proximity with the sample. Whilst the STM technique does achieve high resolution displacement detection, it requires the sample to be conducting and electrically connected. This prevents the investigation of many samples without first coating them in gold, which is not always desirable or practical.

To overcome this problem we have designed and fabricated a new type of SHPM based on piezoresistive atomic force microscopy (AFM). Other related methods have recently been suggested, one employing shear force detection using

additional piezoelectric plates [5] and another using an optical AFM technique [6]. The advantage of our piezoresistive method is that it is fully integrated on one chip and requires no external displacement sensing element, which is a major advantage when working in a low-temperature environment.

Piezoresistive AFM cantilevers, first demonstrated by Tortonese *et al* [7], are commonly fabricated from p-type Si due to its ease of fabrication and strong piezoresistive response in certain crystallographic directions [8]. Our piezoresistive cantilever requires a high-mobility  $\text{Al}_{0.3}\text{Ga}_{0.7}\text{As}/\text{GaAs}$  two-dimensional electron gas (2DEG) to be grown at the surface of the cantilever for the fabrication of a low-noise Hall probe. To achieve this, the piezoresistive cantilever must also be fabricated from GaAs or an  $\text{Al}_x\text{Ga}_{1-x}\text{As}$  alloy. Bulk GaAs has been shown to be an unsuitable material for sensitive piezoresistive detection due to its characteristically low piezoresistive coefficient [9], but the ternary alloy  $\text{Al}_x\text{Ga}_{1-x}\text{As}$  can be tailored to give large piezoresistive coefficients by varying the Al content. In  $\text{Al}_x\text{Ga}_{1-x}\text{As}$  there are four different mechanisms which lead to piezoresistivity, three of which are independent of the crystal direction [10]. The main two mechanisms which we believe contribute to a change in resistivity of our sensor are, firstly a pressure induced transition

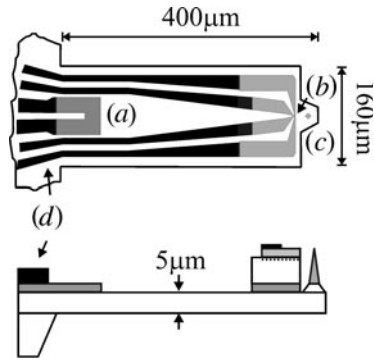


**Figure 1.** Plan and side view of our SHPM cantilever (vertical axis not to scale). The piezoresistor (a) is fabricated at the cantilever base. The Hall probe (b) and the tip (c) are fabricated at the very end of the cantilever. The Hall probe and the piezoresistor are electrically contacted via Au/Ge alloyed contacts (d).

from a direct to an indirect band gap and secondly the pressure induced freezing-out of electrons to deep level impurity states, known as DX centres, both of which are independent of the crystal orientation. The first mechanism is expected to be strong for aluminium atomic fractions near  $x = 0.4$  when the band gap undergoes a direct to indirect transition and the low mobility X band minima drop below the high mobility  $\Gamma$  minimum [10]. By heavily doping our piezoresistive layer near  $x = 0.4$ , an applied stress should result in strong intervalley scattering and a large change in resistivity. The second mechanism arises in  $n\text{-Al}_x\text{Ga}_{1-x}\text{As}$  due to deep donor states known as DX centres. At aluminium fractions  $>0.15$ , these donor states rise in energy above the  $\Gamma$  minimum. These DX centres can trap electrons from the adjacent 2DEG with the application of stress and alter the resistivity of the AlGaAs. The combination of these two effects should lead to a very large piezoresistive response. We indeed find this to be the case and large piezoresistive responses have been measured on  $2.5\ \mu\text{m}$  thick  $n^+\text{-Al}_{0.4}\text{Ga}_{0.6}\text{As}$  ( $1 \times 10^{19}\ \text{cm}^{-3}$  Si doped) epilayers, we find that for the [011] direction,  $\pi_{11}(300\ \text{K}) = 1.35 \times 10^{-9}\ \text{Pa}^{-1}$ . The other two mechanisms, a stress induced variation of the effective mass and a stress *gradient* induced change to the piezoelectric bound charges, we presume to be small compared to the other two.

## 2. Design and fabrication

Our cantilever design is shown in figure 1; the cantilevers are  $5\ \mu\text{m}$  thick and have a length of  $400\ \mu\text{m}$  and a width of  $160\ \mu\text{m}$ . The plan view shows the two primary sensors required for the dual magnetic and topographic imaging. The first sensor, a Hall cross situated near the very end of the cantilever, is electrically contacted via the four gold leads at either side of the cantilever. The piezoresistor is placed at the base of the cantilever where bending stresses are at a maximum. At the very end of the cantilever is a sharp ( $<100\ \text{nm}$  diameter) AFM tip which, by inclining the cantilever, is used to map the sample surface.

The epilayer structure used for our cantilever is sketched in figure 2. The material was grown by MBE at  $600\ ^\circ\text{C}$ . The three uppermost layers, the  $17\ \text{nm}$  GaAs cap layer, the  $40\ \text{nm}$   $n\text{-Al}_{0.3}\text{Ga}_{0.7}\text{As}$  and the  $40\ \text{nm}$  undoped  $\text{Al}_{0.3}\text{Ga}_{0.7}\text{As}$  spacer

layer, are designed to form a high-mobility 2DEG from which the Hall probe is fabricated. The two-dimensional electron gas is formed  $\sim 100\ \text{nm}$  below the surface at the interface between an undoped  $\text{Al}_{0.3}\text{Ga}_{0.7}\text{As}$  spacer layer and the  $1\ \mu\text{m}$  GaAs buffer layer, which allows high resolution magnetic imaging to be achieved. The next sequence of layers, the  $1\ \mu\text{m}$  undoped GaAs layer,  $0.5\ \mu\text{m}$  undoped superlattice and a further  $0.5\ \mu\text{m}$  undoped GaAs layer, are designed as a ‘buffer’ region, to electrically isolate the 2DEG layer from the piezoresistive  $n^+\text{-Al}_{0.4}\text{Ga}_{0.6}\text{As}$  layer situated beneath it. The superlattice is grown from a 20 period  $(2.5\ \text{nm})\text{GaAs}/(25\ \text{nm})\text{Al}_{0.3}\text{Ga}_{0.7}\text{As}$  series of layers. Beneath the buffer region is the  $3\text{--}4 \times 10^{18}$  Si-doped  $n^+\text{-Al}_{0.4}\text{Ga}_{0.6}\text{As}$  piezoresistive layer which has been grown with an Al fraction of  $x = 0.4$  to maximize the piezoresistive response of the cantilever.

The cantilever was fabricated using a combination of selective and non-selective wet etches. The Hall probe is first defined using the non-selective etchant  $\text{H}_2\text{O}:\text{H}_2\text{O}_2:\text{H}_2\text{SO}_4$  in a 1000:8:1 volume ratio to a depth of  $\sim 50\ \text{nm}$  (figure 3(b)). Two further non-selective etches ( $\text{H}_2\text{O}:\text{H}_2\text{O}_2:\text{H}_2\text{SO}_4$  160:8:1 volume ratio) are performed to define the piezoresistor (figures 3(c) and (d)). Au/Ge contacts are evaporated onto the active regions and alloyed at  $420\ ^\circ\text{C}$  to make an Ohmic contact to the piezoresistor and subsequently annealed at  $350\ ^\circ\text{C}$  for the shallow 2DEG ohmic contacts (figure 3(e)). The cantilever is then defined using a deep mesa etch beyond the  $\text{Al}_{0.4}\text{Ga}_{0.6}\text{As}$  etch stop.

At this stage a sharp tip is micromachined at the very end of the cantilever (figure 3(f)). It has been shown that sharp ( $\sim 50\ \text{nm}$  diameter) tips can be fabricated in GaAs using an anisotropic  $\text{H}_3\text{PO}_4$ -based etch [11]. In previous studies, however, the GaAs substrate was etched for many micrometres ( $>20\ \mu\text{m}$ ) which was unsuitable for our cantilever due to its limited ( $<7\ \mu\text{m}$ ) thickness. Our method is similar to this earlier work but was modified to achieve a sharp tip within  $3.5\ \mu\text{m}$  of etching. A  $7\ \mu\text{m}$  square photoresist mask was aligned along the (010) direction and etched in a  $\text{H}_2\text{O}:\text{H}_2\text{O}_2:\text{H}_3\text{PO}_4$  solution in a 1:1:12 volume ratio at  $0\ ^\circ\text{C}$ . The etch rate was found to be  $\sim 0.5\ \mu\text{m}\ \text{min}^{-1}$ . After etching for 4–5 min a sharp tip of  $2\text{--}2.5\ \mu\text{m}$  height was defined. The lower portion of the tip is constructed from shallow {110} facets and the upper portion is made up of steep {105} facets giving a high aspect ratio tip as can be seen in figure 4(b).

Once the tip is defined the cantilever is then released from the substrate (figure 3(g)). This is achieved using a fast non-selective etch ( $\text{H}_2\text{O}:\text{H}_2\text{O}_2:\text{H}_2\text{SO}_4$  1:8:1 ratio) from the backside of the substrate to within  $60\ \mu\text{m}$  of the front side surface. An  $\text{NH}_4\text{OH}/\text{H}_2\text{O}_2$  ( $\text{H}_2\text{O}_2$  plus a few drops of  $\text{NH}_4\text{OH}$ ) selective etch is then used at a pH of 8.3 giving an etch rate of  $\sim 3\ \mu\text{m}\ \text{min}^{-1}$  with a GaAs/ $\text{Al}_{0.4}\text{Ga}_{0.6}\text{As}$  selectivity of 10 to release the cantilever.

The finished cantilevers were then mounted on custom chip carriers designed for our low-temperature SHPM system and ultrasonically bonded to the chip carriers using  $12\ \mu\text{m}$  gold wire.

## 3. Characterization

The resolution of the AFM component of our SHPM system is determined in the  $x, y$  directions by the physical size of the

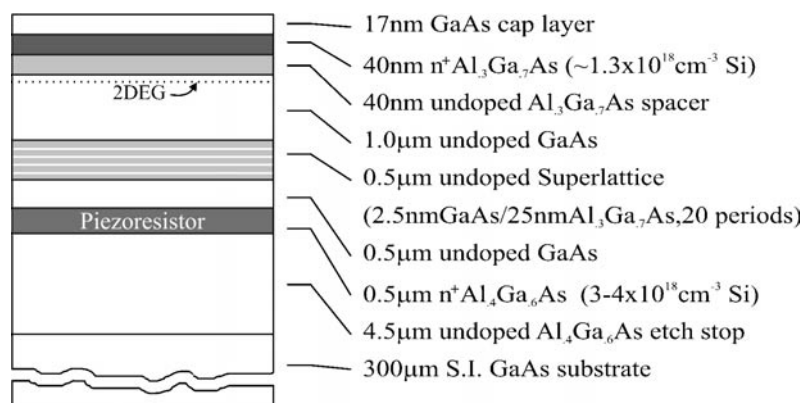


**Figure 2.** Sketch of the epilayer structure of the III-V wafer.

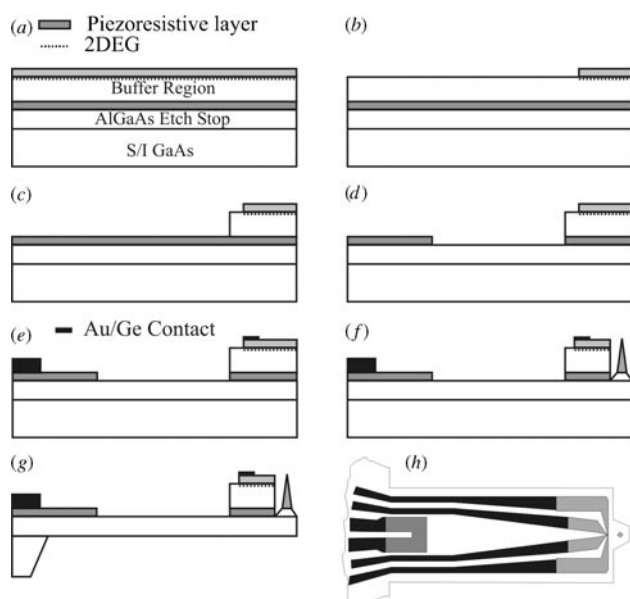


**Figure 3.** The wafer (a) is first etched  $\sim 50$  nm (b) to define the Hall probe. The second etch (c) then exposes the piezoresistive layer which is then patterned (d) with a further etch into the  $\text{Al}_{0.4}\text{Ga}_{0.6}\text{As}$  etch stop. Gold/germanium contacts are then deposited (e) to contact the two devices. A deep etch is performed to define the cantilever and the final front side processing step is to define the tip (f). The cantilever is then released from the substrate using a fast non-selective etch and finally a fast selective etch (g) to the bottom side of the  $\text{Al}_{0.4}\text{Ga}_{0.6}\text{As}$  etch stop (vertical axis not to scale).

tip which is  $<100$  nm. For the  $z$  direction it is determined by the cantilever's minimum detectable deflection. This is a measure of the cantilever's maximum vertical resolution, which is limited by its sensitivity and the noise within the measurement system. The sensitivity is determined by the piezoresistive coefficient of the material and the cantilever geometry. The noise in an AFM measurement system is intrinsically limited by the thermo-mechanical noise of the cantilever [12]. It is possible with the use of optical AFM methods to actually achieve this thermo-mechanical noise limit [12], though for piezoresistive cantilevers the sensitivity is degraded by  $1/f$ , thermal Johnson and pre-amplifier noise.  $1/f$  noise can be avoided by measuring at frequencies above 100 Hz and amplifier noise is relatively small, making Johnson noise the main source of noise in our AFM detection apparatus.

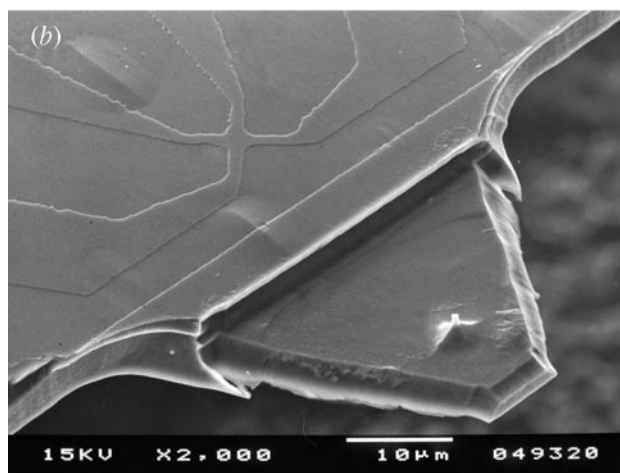
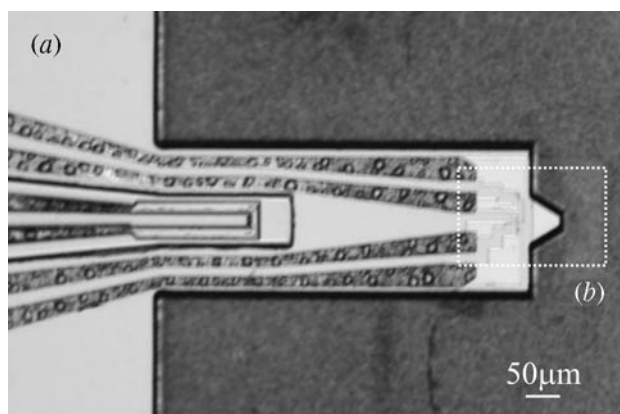


**Figure 4.** (a) Optical micrograph of a fabricated cantilever showing both the piezoresistor and the Hall probe and (b) an SEM image of the end of an integrated cantilever. At this magnification the tip and Hall probe are clearly visible. The Hall probe junction width is  $\sim 1.5$   $\mu\text{m}$ . The high aspect ratio tip can be seen, formed from the  $\{105\}$  facets.

For our cantilevers, with a series resistance of 20 k $\Omega$ , a typical minimum detectable deflection of 10 pm  $\text{Hz}^{-1/2}$  (300 K) is calculated.

The spatial resolution of the Hall probe component of our SHPM is determined in the  $x, y$  directions by the physical size of the Hall probe which in our case is  $<1.5$   $\mu\text{m}$  in figure 4(b). The magnetic field resolution is characterized

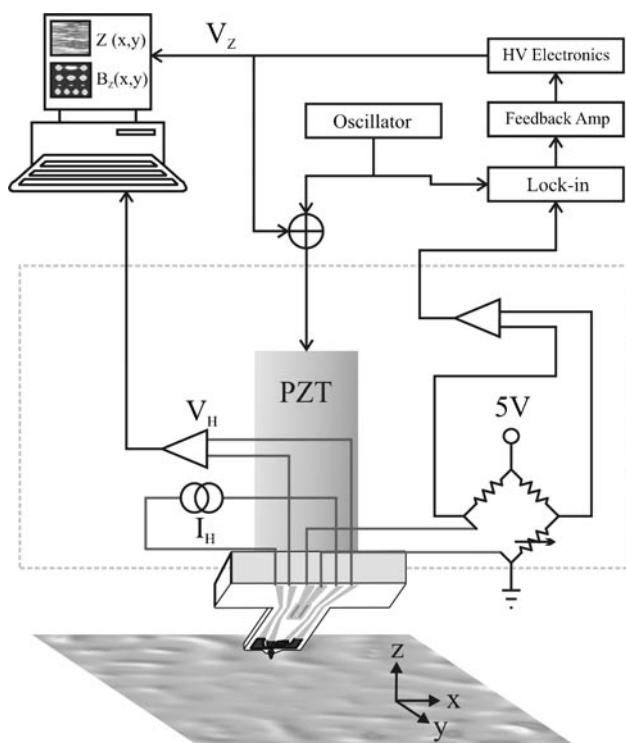


**Figure 5.** Schematic of the piezoresistive AFM-SHPM measurement system.

by the minimum detectable field, which is a measure of the minimum field the Hall probe can detect whose response is equivalent to the intrinsic noise in the voltage leads. The minimum detectable field is also dependent upon the Hall coefficient and the maximum current,  $I_{\max}$ , which can be passed through the current leads. For  $1 \mu\text{m}$  Hall probes,  $I_{\max} \leq 4 \mu\text{A}$  at 300 K rising to  $20 \mu\text{A}$  at 77 K, and currents greater than  $I_{\max}$  significantly increase the  $1/f$  noise. The Hall coefficient for all our probes is roughly constant at  $3000 \Omega \text{T}^{-1}$ .

#### 4. Measurements

Measurements were carried out using a standard SHPM head with a few modifications to the electronics to allow the use in AFM operation as shown in figure 5. The cantilever was mounted at the end of the piezotube and tilted  $2\text{--}4^\circ$  with respect to the sample. The piezoresistive response was detected using a Wheatstone bridge biased at 5 V which was then amplified with an ultra-low-noise pre-amplifier (AD625) with a gain of 100 and detected using a lock-in amplifier. Using the calibrated deflection of the piezotube as a function of applied voltage, the sensitivity of the cantilevers could be measured and was found to be  $\Delta R/(R\Delta z) = 2 \times 10^{-6} \text{ \AA}^{-1}$  at 300 K. With a drive amplitude of 1 nm the resonant frequency of our cantilevers varied between 18–21 kHz and  $Q$  factors of 300–500 were measured in an atmosphere of air.  $Q$  factors rose to  $>10000$  in a good vacuum ( $<10^{-5}$  mbar) as can be seen in figure 6. Also, in figure 6 it can be seen that the response at 77 K is very similar to that at 300 K showing similar sensitivity for the different temperatures. The shift in resonant frequency can

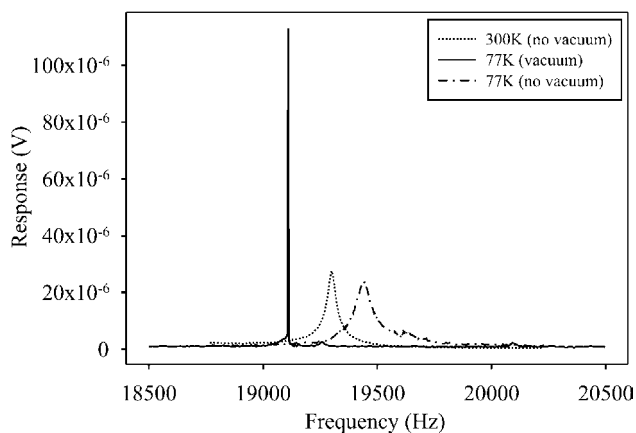


**Figure 6.** Resonant response of our cantilever under different ambient conditions.

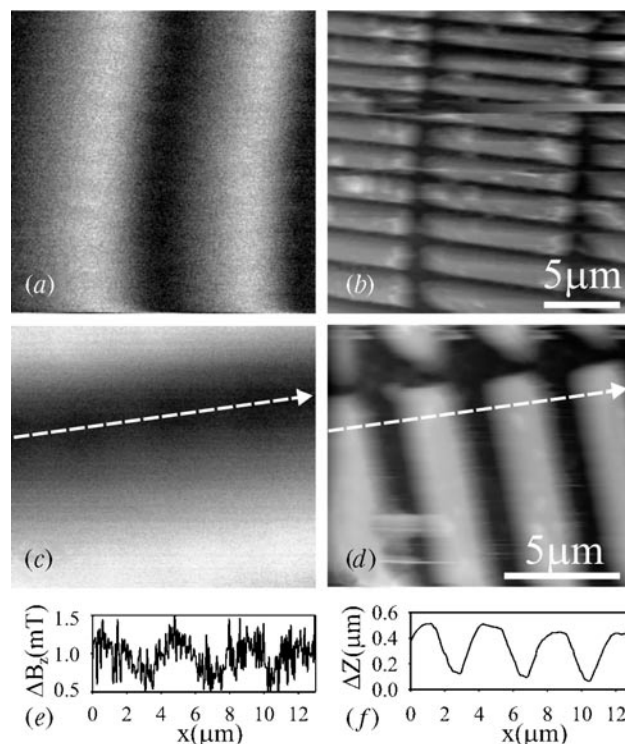


**Figure 7.** Room temperature magnetic (a) and topographic (b) scans of an array of NiFe rectangles (greyscale spans  $\sim 6$  mT (a) and  $\sim 150$  nm (b)). Scans of the same sample in a perpendicular direction at 77 K ((c) and (d)), with line scans ((e) and (f)) in the directions indicated in (c) and (d) (greyscale spans  $\sim 6$  mT (c) and  $\sim 250$  nm (d)).

be attributed to the temperature and pressure dependence of the cantilever force constant.

Figure 7 shows topographic and magnetic scans of a two-dimensional array of unmagnetized NiFe rectangles at room temperature and 77 K. The array, comprising  $2 \mu\text{m} \times 10 \mu\text{m}$  NiFe rectangles with a height of 250 nm and a spacing of  $1 \mu\text{m}$ , was imaged in non-contact AFM mode whilst the local induction was measured simultaneously. The room temperature topographic scan (figure 7(b)) clearly shows the rectangles in a periodic array. The magnetic image (figure 7(a)), however, is less clear due to the Hall sensor spatial resolution being too low ( $\sim 1.5 \mu\text{m}$ ) to resolve the

magnetic domain structure in the multi-domain rectangular bars. The resulting image shows an average of the domain structure giving the light and dark stripes shown. Similarly at 77 K, the topographic image (figure 7(d)), which was scanned in a direction perpendicular to those of figures 7(a) and (b), clearly shows the rectangular grating but again the corresponding magnetic image (figure 7(c)) shows an average of the field produced by the domains in the NiFe rectangles, although some residual detail is observed in the line scan indicated in figure 7(e).

## 5. Conclusion

We have described the fabrication and characterization of a III–V cantilever designed for AFM-tracking scanning Hall probe microscopy. We have shown that by using the ternary alloy  $n^+Al_{0.4}Ga_{0.6}As$  as a piezoresistive material, high displacement sensitivity, in excess of some p-type Si cantilevers, can be achieved. We also demonstrate how a low-noise micron-size Hall probe and a sharp AFM tip can be fully integrated onto a single cantilever. We finally demonstrate the sensors ability to simultaneously scan topographically and magnetically with images of arrays of NiFe rectangles at both room and low temperatures.

## Acknowledgment

The authors would like to acknowledge the financial support of EPSRC (grant no GR/M76119).

## References

- [1] Martin Y and Wickramasinghe H K 1987 *Appl. Phys. Lett.* **50** 1455
- [2] Chang A M, Hallen H D, Harriot L, Hess H F, Loa H L, Kao J, Miller R E and Chang T Y 1992 *Appl. Phys. Lett.* **61** 1974
- [3] Oral A, Bending S J and Henini M 1996 *Appl. Phys. Lett.* **69** 1324
- [4] Sandhu A, Masuda H, Kurosawa K, Oral A and Bending S J 2001 *Electron. Lett.* **37** 1335
- [5] Schweinbock T and Weiss D 2000 *J. Appl. Phys.* **87** 6496
- [6] Chong B K, Zhou H, Mills G, Donaldson L and Weaver J M R 2001 *J. Vac. Sci. Technol. A* **19** 1769
- [7] Tortonese M, Yamada H, Barrett R C and Quate C F 1991 *Proc. Transducers 91 (IEEE)* p 448
- [8] Tufte O N and Stelzer E L 1963 *J. Appl. Phys.* **34** 313
- [9] Dehe A, Fricke K, Mutamba K and Hartnagel H 1995 *J. Micromech. Microeng.* **5** 139
- [10] Hjort Klas, Soderkvist Jan and Schweitz Jan-Ake 1994 *J. Micromech. Microeng.* **4** 1
- [11] Yamaguchi K and Tada S 1996 *J. Electrochem. Soc.* **143** 2616
- [12] Smith D P E 1995 *Rev. Sci. Instrum.* **66** 3191